Laser-driven heterogeneous catalysis: efficient amide formation catalysed by Au/SiO_2 systems

Antonio Pineda,[a] Leyre Gomez,[b] Alina M. Balu,[a] Victor Sebastian,[b] Manuel Ojeda,[a] Manuel Arruebo,[b] Antonio A. Romero,[a] Jesus Santamaria[b] and Rafael Luque*[a]

[a]Department of Organic Chemistry, Marie Curie Building, Ctra Nnal IV-A Km 396, University of Córdoba, E14014 Córdoba, Spain. E-mail: q62alsor@uco.es [b]Department of Chemical Engineering and Aragon Institute of Nanoscience (INA), Campus Río Ebro – Edificio I+D, C/Mariano Esquillor s/n, University of Zaragoza, 50018 Zaragoza, Spain. E-mail: jesus.santamaria@unizar.es

A proof of concept of laser-assisted heterogeneously catalysed processes at room temperature using silica supported gold nano- particles is reported. Au/SiO_2 nanoparticles were laser-irradiated at 532 nm (SPR maximum absorbance) to catalyse the selected reaction, namely the production of 4-benzoylmorpholine from benzaldehyde and morpholine *via* amide formation, for which quantitative yields to the target amide were obtained after 3–5 h of reaction. The protocol could also be extended to a tandem oxi- dation/amidation process which shows the potential of the pro- posed approach for the promotion of liquid-phase organic reactions at room temperature.

Metal nanoparticles can serve as both local nanoscale-heat sinks and catalysts to drive heterogeneous catalytic reactions at room temperature in the absence of macroscopic heating. This could in principle be done by a laser-induced selective exci- tation of the surface plasmon resonance of nanoparticles at a particular wavelength. In this way, gas[1,2] and liquid[3–5] phase heterogeneous catalytic processes have been reported to be accelerated by using laser excitation on various nanoparticles used as catalysts. In view of these principles, Trammel *et al*. accelerated the catalytic rate of the hydrolysis of methyl parathion by a factor of 2 with a simple laser irradiation at 532 nm of the plasmon absorption band of gold nanoparticles in a Cu- decorated Au nanoparticles catalyst.[6] The selective oxidation of *sec*-phenethyl and benzyl alcohols to acetophenone and benz- aldehyde, respectively, comparing the use of different optical (laser and light emitting diode) and microwave energy sources, was also described using gold nanoparticles as catalysts.[7]

Photonic nanoparticles have a strong surface plasmon resonance (SPR) absorption in the visible region due to the collective oscillation of free electrons in the conduction band.[8] Incident photons are converted into phonons and generate lattice vibrations which are both responsible for heating up the nanoparticles. Hence, this absorption of the incident radiation generates heat which is rapidly dissipated in the immediate surroundings. This heat can even produce vaporisation of the solvent and cavitations in the proximity of nanoparticles. Localised heating at the nanoscale is usually achieved by using pulsed lasers because the duration of the optical excitation is shorter than the time scale needed for the heat to diffuse the distance of the average particle–particle spacing.[9] Continuous wave lasers can also be used; however, in those cases, heat is transmitted far away from the nanoparticle.[9] This temperature increase is proportional to the second power of the nanoparticle radius.[10] Larger nanoparticles would therefore be prefer- able to achieve larger heating gradients; however, gold nanoparticles are catalytically efficient only at reduced sizes (about 5 nm or less).[11] In addition, SPR responsible nanoparticles might undergo acoustic vibration of their lattices after laser absorption and consequently melting, evaporation and fragmentation phenomena.[12] In this way, there are several limitations in terms of laser utilisation to be coupled with nanoparticles to avoid their degradation and activity loss in the course of laser-promoted chemistries.

For the particular case of nanoparticulated gold (a soft Lewis acid), its use as a catalyst in organic reactions including additions, cyclisations, rearrangements, couplings, oxidations, and hydrogenations has been recently reviewed by Corma *et al*.,[13] highlighting the extensive range of applications of gold nanoparticles in catalytic organic chemical processes. The catalytic activity of gold nanoparticles markedly depends on their size, shape,

dispersion, support and the deposition method used in their preparation as well as on the role of the interface catalyst–support. In the search for energy efficient processes, gold nanoparticles can also allow significantly reduced reaction temperatures in catalytic reactions compared to those utilised in conventional processes.[11] Nevertheless, their combi- nation with a localised heating achievable under laser irradiation might enhance even more the energetic efficiency, thus accelerating the rates of reaction in catalytic processes even at room temperature.

In view of these premises, we describe herein a proof of concept of laser-assisted heterogeneously catalysed processes at room temperature using silica supported gold nanoparticles. Au–silica was laser-irradiated at 532 nm (SPR maximum absorbance) to catalyse the selected reaction, namely the pro- duction of 4-benzoylmorpholine from benzaldehyde and morpholine *via* amide formation. Amide formation avoiding poor atom economy reagents was the top priority and most relevant transformation for pharmaceutical manufacturers as defined by the ACS GCI Pharmaceutical Round Table in 2007.[14] Mor-pholine derivatives are in fact interesting intermediates in the synthesis of many pharmaceuticals and they have been applied as analgesics, local anaesthetics, and respiratory and vasomotor stimulants.[15]

The proposed focused laser-assisted protocol allows a rapid heating and easy and remote controllability, which can speed up reaction kinetics without heating all the thermal mass of the system. In addition to the potential energy savings achieved with localised laser-driven heating, thermal heterogeneities, which are observed in conventional convective heating, can also be avoided, being such an approach of special interest for chemical reactions of high energies of activation and slow reaction rates.

EXPERIMENTAL

Benzaldehyde (≥99.5%), benzyl alcohol (≥99.5%), morpholine (≥99.0%), tetrahydrofurane, THF (≥99.9%), (3-aminopropyl)- triethoxysilane (≥98%), tetraethyl orthosilicate (>98%), gold(III) chloride hydrate (≥99.999%), a tetrakis(hydroxymethyl)phosphonium chloride solution (80% in water) and H_2O_2 (aqueous 50 wt%, v/v) were purchased from Sigma Aldrich and used as received.

Catalyst preparation

Silica nanoparticles decorated with gold seeds were prepared by following the protocol previously described for the seeding step in the preparation of gold nanoshells by Bardhan *et al*.[16] In brief, silica nanoparticles were initially prepared by following the synthesis described by Stöber *et al*.[17] The surface of the resulting nanoparticles was grafted with amino groups *via* silane coupling. Gold nanoparticles were separately prepared and bound to the amino-functionalized silica. The excess of gold nanoparticles or unbound seeds was removed by successive washing steps.

Catalyst characterisation

The shape, size, particle size distribution, and microstructure of the nanoparticles were studied by using a T200 Philips Tecnai Transmission Electron Microscope (TEM) operated at

200 kV. At least one hundred nanoparticles were measured to evaluate the mean diameter of the particles and the standard deviation. The data were fitted with a log–normal distribution function and the logarithmic standard deviation was obtained for all the samples. Hydrodynamic sizes were evaluated in a 90 Plus dynamic light scattering (DLS) apparatus (Brookhaven Instruments Corp.). An ultraviolet visible spectrophotometer (Jasco V670) was used to evaluate the extinction (absorption and scattering) bands of the catalysts in the different solvents.

Spherical gold nanoparticles show their characteristic SPR absorption band at ~520–550 nm depending on their sizes. For that reason, we used a solid state 532 nm green laser (0.5 W) (Changchun New Industries Optoelectronics Tech. Co., Ltd) operating in continuous wave mode to excite the as synthesized plasmonic nanoparticles. The laser was placed at 8 cm from the surface of the solvent rendering a fluence of 2.1 W cm^{-2} measured using a photodiode sensor (Ophir Optronics).

Amidation reaction

In a typical reaction, 0.025 g of the catalyst was placed in a pyrex tube together with 19 mL of THF, 0.2 mL of benz- aldehyde, 0.2 mL of morpholine, 1 mL of H_2O_2 and 0.01 g of KOH (under otherwise stated conditions). Then the reaction mixture was illuminated with the laser source for the desired period of time, from which samples were periodically withdrawn, subsequently filtered off and analysed by GC and GC/ MS using an Agilent 6890N GC model equipped with a 7683B series autosampler, fitted with a DB-5 capillary column and an FID detector. Response factors of the reaction products were determined with respect to the original starting materials from GC analysis using known compounds in calibration mixtures of specified compositions.

In the case of the tandem process, double quantities of H_2O_2 (2 mL) were added dropwise to facilitate the oxidation of benzyl alcohol (0.2 mL) to benzaldehyde that subsequently reacted with morpholine to give the desired amide in high yields.

Reusability experiments performed for the catalysts were carried out as follows: upon reaction completion in the first run, the catalyst was filtered off, washed thoroughly with acetone and oven-dried at 100 °C prior to its reuse in the reac- tion. For the three uses experiment, double quantities of the reaction mixture, reagents (0.4 mL benzaldehyde or benzyl alcohol, 0.4 mL amine) and the catalyst (0.05 g) were utilised to maximise the quantity of the catalyst available and mini- mise the effect of catalyst loss after each reuse.

RESULTS AND DISCUSSION

The synthesized spherical gold nanoparticles comprising mul- tiply twinned crystals showed a particle-size distribution centred at 1.85 ± 0.55 nm. Fig. 1 shows the distribution of the gold seeds on the surface of the dense silica nanoparticles used as supports. Gold nanoparticles are strongly attached to the surface of the amino-functionalised silica due to the chemical bond between the electron-rich nitrogen present in the primary amines of the silica and the gold orbitals *via* their the solvent used (THF) is shown to demonstrate its lack of absorption at the light wavelength used (532 nm).

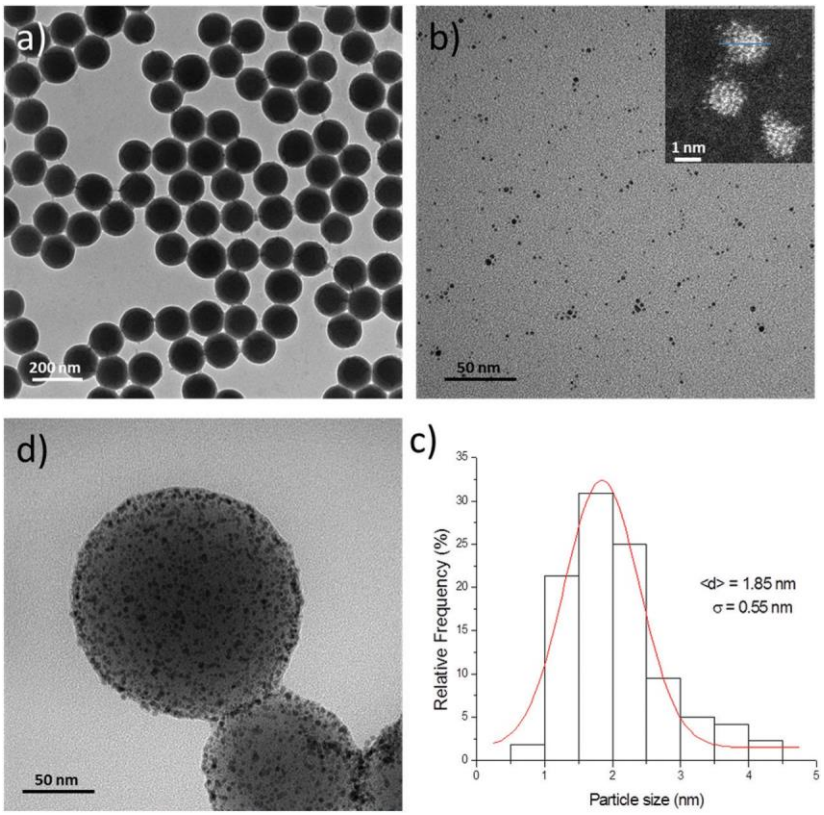

Fig. 1 TEM photographs describing the morphology of the catalyst: (a) silica nanoparticles used as a support, (b) Au seeds and (c) Au nanoparticles decorating the surface of the silica after amino–silane coupling. (d) Histogram (N = 220) showing the particle-size distribution of the Au nanoparticles.

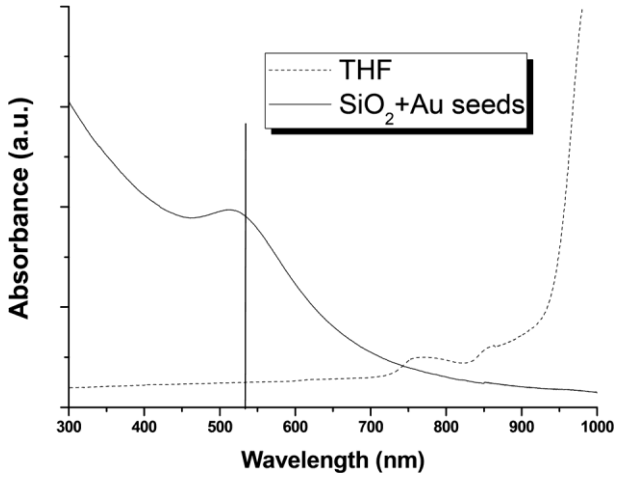

Fig. 2 UV-VIS spectra of the Au/SiO_2 nanoparticles used as catalysts. For com- parison the spectrum of

Fig. 2 shows the weak absorption of the gold nanoparticles characteristic of their small size (1.85 ± 0.55 nm). According to the Mie theory, the scattering for such small nanoparticles canbe neglected and the initial rising shoulder at wavelengths below 500 nm can be attributed to interband transitions.[12]

Only dipole oscillation contributes to the extinction cross- section when the diameter of the gold nanoparticle is much smaller than the wavelength of the radiation. When the nano-particles are arranged in arrays, the interactions between indi- vidual dipole plasmons can further increase this extinction. Fig. 2 also highlights that the solvent utilised in the organic reaction does not absorb the incident light (532 nm); only nanoparticles are responsible for the localised heating. Upon laser irradiation, the temperature of the reaction mixture remained below 25 °C even after 24 h, indicating that the heat generated by the gold nanoparticles was rapidly dissipated by the solvent.

The reaction selected as a proof-of-concept for the proposed approach was the preparation of 4-benzoylmorpholine (product A) from benzaldehyde and morpholine (Scheme 1).

This product was recently reported to be formed by polymer-incarcerated carbon black Au nanoparticles (PICB-Au) catalysis at 40 °C in over 12 h of reaction,19 being one of the most challenging substrates to couple from the reported work. Fig. 3 summarises the comparative experiments carried out under the different investigated conditions with Au/SiO2, demonstrating that 4-benzoylmorpholine could be efficiently produced at room temperature under laser-assisted conditions in 4–5 h of reaction. This time reduction compared to previous literature highlights the economical impact of this energy-saving approach.

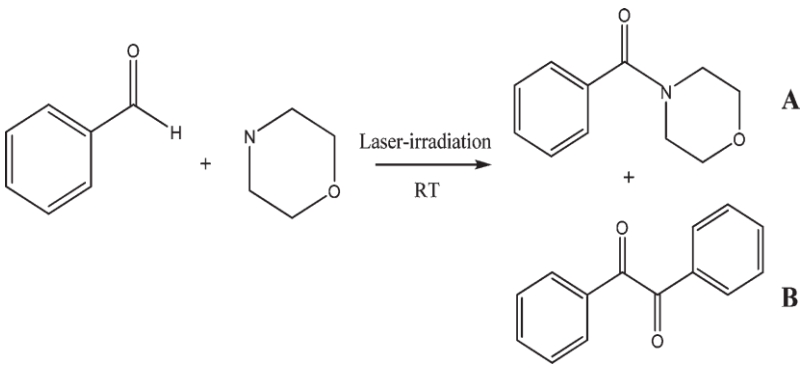

Scheme 1 Laser-driven amide formation between benzaldehyde and morpho- line at room temperature.

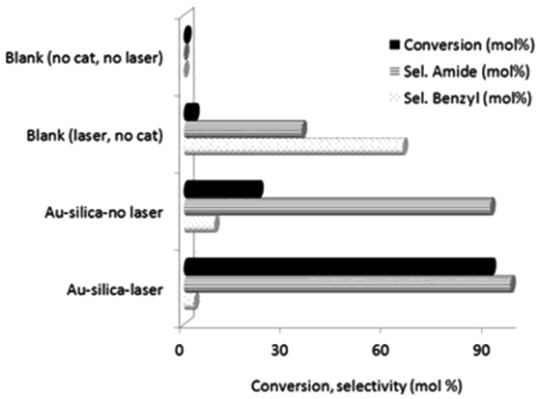

Fig. 3 Comparative experiments in the amidation of benzaldehyde and mor- pholine at RT conducted under identical conditions. Reaction conditions: 0.2 mL benzaldehyde, 0.2 mL morpholine, 19 mL THF, 1 mL H_2O_2, 0.01 g KOH and
0.025 g Au–silica catalyst, 4 h of reaction, 25 °C.

Blank runs (with laser without a catalyst and with a catalyst without laser) gave almost negligible activity, with only the laser-absent Au-catalysed reaction at RT providing poor yields (<30%) after 6 h of reaction (Fig. 3). Interestingly, a convention- al thermal experiment at 60 °C catalysed by Au–SiO_2 provided fairly similar results to those obtained under laser-assisted conditions at RT (results not shown), in good agreement with our proposed theories of laser localised-heating under the investigated conditions. Interestingly, energy measurements further proved that the estimated energy consumption of the laser-assisted process after 5 h (<0.01 kWh) was remarkably inferior to the obtained 0.1 kWh of a comparable 5 h thermal reaction (60 °C) experiment run in a 650 W hot plate (for full details, see the ESI†).

The reaction was also found to be amenable to other amines, namely alpha-methyl benzylamine (99% conversion, 98% selectivity to the corresponding amide after 3 h of reaction) and benzylamine (97% conversion, 95% selectivity to *N*-benzylbenzamide after 5 h of reaction). In the latter case, *N*-benzylbenzamide formation was low at RT and was only efficiently formed thermally from benzylamine (at 60 °C in the absence of catalyst without the need for the laser-assisted methodology) or at RT under laser-assisted conditions under otherwise identical reaction conditions to those of Fig. 3.

Furthermore, while this particular amide formation reaches conversion levels of *ca.* 80–85% (at >98% selectivity to benzamide) after 1 h at 60 °C but did not progress any further to completion, conversions in the systems could be pushed to quantitative yields of *N*-benzylbenzamide by means of the pro- posed laser-assisted methodology. For all cases, atom efficien- cies worked out were between 0.56 (for the reaction between benzaldehyde and morpholine) and 0.60, taking into account all reagents including THF as a solvent, hydrogen peroxide and KOH, which is in the range of 55–60%.

It is worth pointing out at this stage that a series of Au nanoentities (*e.g.* hollow and solid Au NPs, Au nanorods) as well as supported Au NPs on various supports (*e.g.* core–shell

nanoparticles, *etc*.) were also investigated in the selected process, with generally low yields to amides obtained in all cases. The selected optimum Au/SiO_2 catalyst was also found to be highly stable and reusable under the investigated conditions, preserving over 90% of its initial activity after 2 re-uses.

The next step forward was the application of this proof of concept reaction to a tandem oxidation/amidation process for amide synthesis from benzyl alcohol and morpholine (Scheme 2).

In a first step, benzyl alcohol was oxidised to benzaldehyde (promoted by the addition of H_2O_2 and the bubbling of molecular oxygen in the system) and then amide formation subsequently takes place. The proposed reaction was found to give *ca.* 38% conversion in 4 h with >99% selectivity to the target product. This and related tandem processes are currently under optimisation in our laboratories to select the best conditions to improve conversions in the systems.

In any case, a further approach to the kinetics of the laser- assisted catalytic system was conducted. Initial and maximum reaction rates were worked out from conversion data profiles (Fig. 4) and results have also been included and compared in Table 1. Unfortunately, the reaction kinetics were rather complex for a full detailed study at this stage in terms of the order of reaction, the rate determining step and related kinetic parameters. Nevertheless, preliminary findings seem to indicate a few interesting points worth further investigation. Generally, the initial rates of reaction were as expected 10 times superior in the laser-assisted catalysed process as compared to those obtained with the Au systems without the laser (Table 1). The laser-assisted reaction in the absence of catalyst provided no appreciable rate of reaction. Importantly, the maximum rates of reaction for the three investigated cases were even more remarkably different (Table 1).

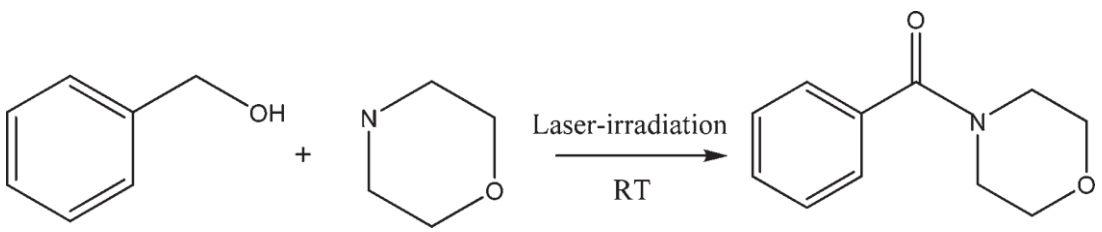

Scheme 2 Laser-driven tandem oxidation/amidation reaction. Benzyl alcohol and benzyl amine to *N*-benzylbenzamide. Reaction conditions: 0.2 mL benzyl alcohol, 0.2 mL morpholine, 19 mL THF, 1 mL H_2O_2, 0.01 g KOH, 2 mL H_2O_2 (added dropwise) and 0.025 g $Au–SiO_2$ catalyst, 4 h of reaction, 25 °C.

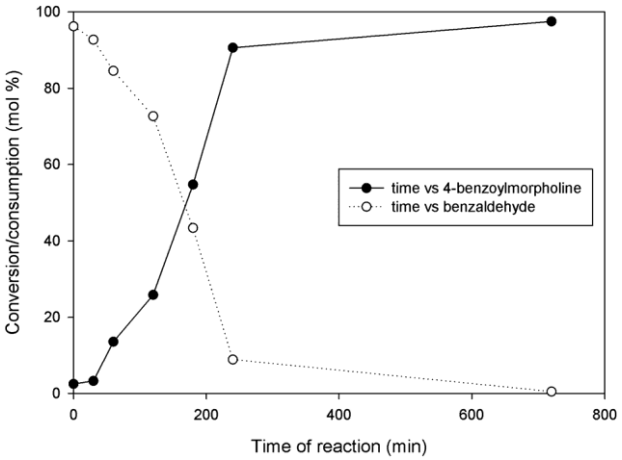

Fig. 4 Reaction profiles of benzaldehyde consumption and product generation in the laser-assisted amidation of benzaldehyde and morpholine. Reaction conditions: 0.2 mL benzaldehyde, 0.2 mL morpholine, 19 mL THF, 1 mL H_2O_2, 0.01 g KOH and 0.025 g Au–silica catalyst, 25 °C. The proposed induction period can be clearly observed at the beginning of the reaction (the first 30–60 min, see the line of 4-benzoylmorpholine formation).

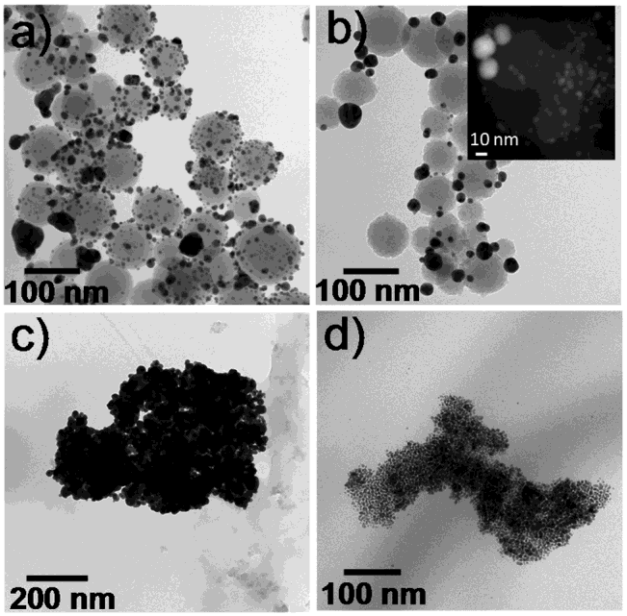

Fig. 5 TEM photographs of the nanoparticles after laser exposure for (a) 15 h of reaction and (b) 24 h of reaction (1 use). Inset: STEM–HAADF image (c) after

Table 1 Rates of reaction in the amidation of benzaldehyde and morpholine (from the results depicted in Fig. 4)[a]

Conditions	Initial rate (mmol min^{-1})	Maximum rate (mmol min^{-1})
Blank (laser, no cat.)	—	2.7×10^{-4}
Au–silica (no laser)	1.5×10^{-4}	0.07
Au–silica (laser)	2.5×10^{-3}	1.28

[a] Reaction conditions: 0.2 mL benzaldehyde, 0.2 mL morpholine, 19 mL THF, 1 mL H_2O_2, 0.01 g KOH and 0.025 g Au–silica catalyst (where appropriate).

A considerable induction period in the reaction can therefore be inferred from these results which might be plausibly explained as a contribution of two important facts. Firstly, and most importantly, kinetics seemed to indicate the likely presence of an inhibitor as the cause of the induction period at the beginning of the reaction. The affinity of amines (*e.g.* pyridine, ethylenediamine, *etc.*) for metal nanoparticles, particularly Pd and Au, is well known.[20] Morpholine (and related investigated amines) may be preferentially adsorbed on the Au NP sites and therefore slow the initial reaction kinetics in the process. Upon a local increase in temperature on the surface of nanoparticles (achieved upon plasmon excitation), the strongly adsorbed amines may desorb from the surface leaving uncoordinatively unsaturated sites to start driving the reaction. The room temperature catalysed Au/ SiO_2 reaction in the absence of laser provided very slow maximum rates of reaction, which essentially support the hypothesised mechanism of restricted availability of active centers (at low temperatures) due to amine coordination. Nevertheless, further studies are currently ongoing to support the present hypothesis with supplemented results that could also offer insights into the reaction mechanism and serve as

was subsequently investigated in detail. Fig. 5 (see also the supporting info) shows the morphology of the catalysts after successive reactions.

Fig. 5a shows the morphology of the nanoparticles after 15 h of reaction (laser exposure) indicating incipient sintering and gold agglomeration in agreement with previous work.[12] After 24 h (Fig. 5b), a large sintering was observed and even bare silica nanoparticles were observed, indicating that the gold seeds migrate across the surface and are clumped together. As Werner *et al.*[21] demonstrated, nanoparticle fusion was seriously affected by the irradiation atmosphere showing larger agglomerations when using oxygen saturated solutions. In our case, the usage of H_2O_2 might also accelerate the coalescence process observed. It is clearly observable that silica is partially dissolved after two consecutive reactions (Fig. 5c, see also the supporting info).

This result is in agreement with the work by Prasad *et al*.[22] which showed silica removal and gold shell disruption after femto-second laser irradiation for hybrid core/shell SiO_2/Au nanoparticles. Control reactions using conventional heating showed also nanoparticle coalescence and clumping (Fig. 5d). Even though the damage caused in the catalysts was clearly observable, the conversion was still very high after two reuses of the same catalyst, indicating that the damage was not extended to all of the catalyst mass. To corroborate this observation, the inset of Fig. 5b shows that a large number of small (<5 nm) gold nanoparticles remain on the catalyst support even after one use. Also, Liu and Mi[23] demonstrated that a few surface layers of nanoparticles are responsible for the absorption of the heat in nanoparticle agglomerates formed by evenly distributed plasmonic nanoparticles; the rest exclusively contribute to heat transfer. This phenomenon can also be an explanation of our experimental observation. In any case, no Au leaching was detected in the solution (as determined by ICP-MS) under the investigated conditions. However, this thermal effect may be minimized by using pulsed lasers instead of continuous wave ones without decreasing the photo- dynamic effect.

A pictorial representation of the remarkable and unique stress wave generation and bubble/shockwave formation in our systems during the selected chemistries under laser excitation is shown in Fig. 6 and as videos in the supporting info. The shockwaves clearly visible during the reaction were accompanied by intense and continuous popping-like sound during the initial minutes of reaction becoming less important after 1–2 h of reaction. This was a common phenomenon observed in both the amidation and the oxidation/amidation tandem process.

A plausible physics-related explanation of the observed phenomenon can be drawn as the conclusion. The incoming laser light optically excites surface plasmons on the metal surface, and the plasmons then decay into “hot” electrons. Because of their high energies, “hot” electrons extend further away from the nanoparticles than electrons with lower energies do. If another atom or molecule that can accept the electron is nearby, the “hot” electron can transfer into that acceptor’s electronic states, in a similar way to that recently demonstrated by Mukherjee *et al.* in the plasmon-induced dissociation of hydrogen molecules on Au.[24]

In heterogeneous catalysis it is not necessary to heat up all the mass of reactants to drive catalytic reactions. By heating exclusively plasmonic nanoparticles responsive to a specific wavelength which causes absorption it is possible to convert it into heat which drives the reaction. In any case, further investigations to extend the proposed protocol to other substrates and related chemistries are currently under way in our laboratories but preliminary

studies point out that the protocol can also be extended to related (*e.g.* couplings) and tandem reactions (oxidation/couplings) under laser-assisted conditions.

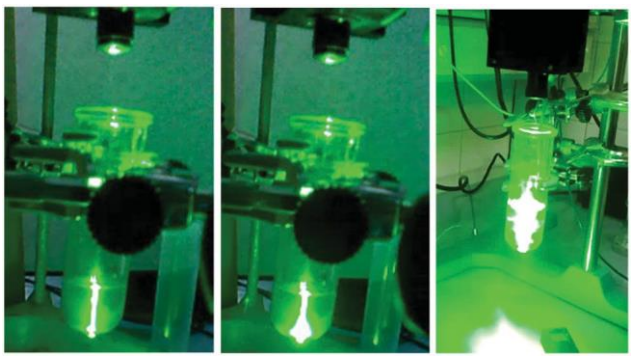

Fig. 6 Digital photographs of different reaction times showing the stress wave generation as well as the bubble/shockwave formation in the course of the organic reaction during laser excitation.

ACKNOWLEDGEMENTS

RL gratefully acknowledges MICINN for the award of a Ramon y Cajal Contract (ref. RYC-2009-04199) and funding from pro- jects CTQ2011-28954-C02-02 (MEC) and P10-FQM-6711 (Consejeria de Ciencia e Innovacion, Junta de Andalucía). MA also gratefully acknowledges the support of the MICINN through the MAT2011-24988 grant. The authors are indebted to and greatly appreciate the assistance of Dr Vitaly Budarin from Green Chemistry at York University (UK) for useful and insightful kinetics calculations and discussions.

REFERENCES

1 W. H. Hung, M. Aykol, D. Valley, W. Hou and S. B. Cronin, *Nano Lett.*, 2010, 10, 1314–1318.
2 J. R. Adleman, D. A. Boyd, D. G. Goodwin and D. Psaltis, *Nano Lett.*, 2009, 9, 4417–4423.
3 T. F. George, Final Report, Rochester University, New York, USA, 1986, http://adsabs.harvard.edu/abs/1986runy.rept G
4 C. J. Bueno Alejo, C. Fasciani, M. Grenier, J. C. Netto- Ferreira and J. C. Scaiano, *Catal. Sci. Technol.*, 2011, 1, 1506–1511.
5 C. Fasciani, C. J. Bueno Alejo, M. Grenier, J. C. Netto- Ferreira and J. C. Scaiano, *Org. Lett.*, 2011, 13, 204–207.
6 S. A. Trammell, R. Nita, M. Moore, D. Zabetakis, E. Chang and D. Andrew Knight, *Chem. Commun.*, 2012, 48, 4121– 4123.
7 G. L. Hallett-Tapley, M. J. Silvero, M. Gonzalez-Bejar, M. Grenier, J. C. Netto-Ferreira and J. C. Scaiano, *J. Phys. Chem. C*, 2011, 115, 10784–10790.
8 P. Mulvaney, *Langmuir*, 1996, 12, 788–800.
9 P. Keblinski, D. G. Cahill, A. Bodapati, C. R. Sullivan and A. T. Taton, *J. Appl. Phys.*, 2006, 100, 054305.
10 A. O. Govorov and H. H. Richardson, *Nano Today*, 2007, 2, 30–38.
11 B. Hvolbaek, T. V. W. Janssens, B. S. Clausen, H. Falsig, C. H. Christensen and J. K.

Nørskov, *Nano Today*, 2007, 2, 14–18.
12 S. Hashimoto, D. Werner and T. Uwada, *J. Photochem. Photobiol., C*, 2012, 13, 28–54.
13 A. Corma and H. Garcia, *Chem. Soc. Rev.*, 2008, 37, 2096–2126.
14 D. J. C. Constable, P. J. Dunn, J. D. Hayler, G. R. Humprey, J. L. Leazer Jr., R. J. Linderman, K. Lorenz, J. Manley,
B. A. Pearlman, A. Wells, A. Zaks and T. Y. Zhang, *Green Chem.*, 2007, 9, 411–420.
15 http://www.huntsman.com/performance_products/Media/m orpholine_(entire_brochure).pdf
16 R. Bardhan, N. K. Grady and N. J. Halas, *Small*, 2008, 4, 1716–1722.
17 W. Stöber, A. Fink and E. Bohn, *J. Colloid Interface Sci.*, 1968, 26, 62–69.
18 A. H. Pakiari and Z. Jamshidi, *J. Phys. Chem. A*, 2007, 111, 4391–4396.
19 J. F. Soule, H. Miyamura and S. Kobayashi, *J. Am. Chem. Soc.*, 2011, 133, 18550–18553.
20 (*a*) K. Aslan, P. Holley and C. D. Geddes, *J. Mater. Chem.*, 2006, 16, 2846–2852; (*b*) R. A. Sperling and W. J. Parak, *Philos. Trans. R. Soc. London, Ser. A*, 2010, 368, 1333–1383.
21 D. Werner, S. Hashimoto, T. Tomita, S. Matsuo and
Y. Makita, *J. Phys. Chem. C*, 2008, 112, 16801–16808.V. Prasad, A. Mikhailovsky and J. A. Zasadzinski, *Langmuir*, 2005, 21, 7528–7532.
22 C. Liu and C. C. Mi, *IEEE Trans. Nanobiosci.*, 2008, 7, 206–214.
23 S. Mukherjee, F. Libisch, N. Large, O. Neumann, L. V. Brown, J. Cheng, J. B. Lassiter, E. A. Carter, P. Nordlander and N. J. Halas, *Nano Lett.*, 2013, 13, 240–247.